Magnetic field induced global paramagnetic response in a Fulde-Ferrell superconducting strip

P. M. Marychev,[1] V. D. Plastovets,[1,2,3] and D. Yu. Vodolazov[1]

[1]*Institute for Physics of Microstructures, Russian Academy of Sciences, 603950, Nizhny Novgorod, GSP-105, Russia*

[2]*Lobachevsky State University of Nizhny Novgorod, Nizhny Novgorod, 603950, Russia*

[3]*Sirius University of Science and Technology, 1 Olympic Avenue, 354340 Sochi, Russia*

(Received 11 June 2020; revised 14 July 2020; accepted 14 July 2020; published 26 August 2020)

We theoretically study the magnetic response of a superconductor/ferromagnet/normal-metal strip in an in-plane Fulde-Ferrell (FF) state. We show that unlike an ordinary superconducting strip, the FF strip can be switched from diamagnetic to paramagnetic and then back to a diamagnetic state by *increasing* the perpendicular magnetic field. Being in a paramagnetic state, the FF strip exhibits a magnetic field driven second-order phase transition from the FF state to the ordinary state without spatial modulation along the strip. We argue that the global paramagnetic response is connected with a peculiar dependence of the sheet superconducting current density on supervelocity in the FF state, and it exists in the nonlinear regime.

DOI: 10.1103/PhysRevB.102.054519

I. INTRODUCTION

The diamagnetic Meissner effect, together with zero resistivity, is the fundamental property of a superconducting state. When one places a superconducting specimen in a weak magnetic field, screening supercurrents expel magnetic flux from the interior of the superconductor, which leads to its diamagnetic response. However, there are experimental observations of the so called paramagnetic Meissner effect (PME) in high-T_c superconductors [1,2] and disks of conventional superconductors [3,4]. But in all these cases, anomalous paramagnetic response was observed only upon cooling in low magnetic fields and was absent upon cooling without an applied field. For granular high-T_c superconductors, the PME can be explained by the presence of the π-junctions [5], while in the other cases the PME is caused by the trapped flux on intrinsic inhomogeneities or the surface [6,7].

Paramagnetic response without the captured flux (vortices) can be realized in the case of unusual Cooper pairing, namely the odd-frequency superconductivity. Odd-frequency pairs formally have negative density that leads to paramagnetic supercurrents and, consequently, local paramagnetism [8]. The odd-frequency superconducting state can be realized in the ferromagnet part of hybrid superconductor/ferromagnet (SF) structures [9], near the normal metal/p-wave superconductor (NS) interfaces [10], and near the surface of d-wave superconductors [11]. A local paramagnetic response of odd-frequency superconductivity was directly observed in a superconductor/ferromagnet/normal-metal (SFN) trilayer [12] via measurement of an enhanced magnetic field in a normal layer. Also, a paramagnetic response of normal metal was seen at ultralow temperatures in the hybrid superconductor/normal metal structure [13], which could be explained by the presence of dilute magnetic impurities leading to odd-frequency superconductivity [14].

In relatively thin SF or SFN strips, the paramagnetic response of odd-frequency superconducting correlations in F or FN layers may exceed the diamagnetic response of the S layer (at a proper choice of material parameters), and the in-plane Fulde-Ferrell-Larkin-Ovchinnikov (FFLO) state could be developed [15,16]. It is modulated along the strip superconducting state, and its existence was originally predicted for bulk superconductors with a spatially uniform exchange field and energy splitting of electrons with opposite spin of order of the superconducting gap [17,18]. In the FF state, the superconducting order parameter has the form of the plane wave [$\propto \exp(i\mathbf{q}_{\mathrm{FF}}\mathbf{r})$], while in the LO state it is the standing wave [$\propto \cos(\mathbf{q}_{\mathrm{LO}}\mathbf{r})$ near T^{FFLO}]. In the pioneer work of Refs. [17,18], it was shown that when the system is in the FF or LO state, it retains the conventional diamagnetic Meissner response at small magnetic fields.

Here we show theoretically that the magnetic response of an SFN strip in an in-plane Fulde-Ferrell state is also diamagnetic at small and large fields, but there is a finite range of fields where the magnetic response is globally paramagnetic. It differs from a global paramagnetic response predicted for small-sized unconventional superconducting disks [19] and thin disks/squares made of an SFN trilayer [20], where it appears due to the finite-size effect and exists only at small fields. We argue that in the case of an SFN strip, a global paramagnetic response is connected with the peculiar dependence of sheet superconducting current density on supervelocity in the FF state, and it appears in the nonlinear regime (when the dependence of superconducting current on the vector potential is nonlinear). The paramagnetic response is accompanied by a magnetic field driven second-order phase transition from an FF-like state to an ordinary state without spatial modulation along the strip. We also find that in the presence of a parallel magnetic field, magnetization curves could be different depending on the direction of $\mathbf{q}_{\mathrm{FF}}$ along the strip, which allows one to determine its direction from magnetic measurements.

II. MODEL

We study magnetic response of an SFN strip with length L and width w made of a superconductor with thickness d_{S}, a

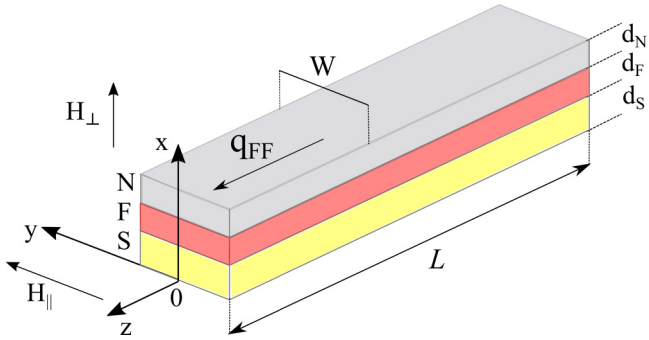

FIG. 1. The schematic representation of the SFN strip placed in parallel and perpendicular magnetic field.

ferromagnet with thickness d_F, and normal metal with thickness d_N (see Fig. 1). In Ref. [16] it was shown that when the ratio of resistivities $\rho_S/\rho_N \gg 1$, the thicknesses of S and N layers are about of coherence length in the superconductor, and the thickness of the F layer is about of coherence length in the ferromagnet. The in-plane Fulde-Ferrell-Larkin-Ovchinnikov state could be realized (in a realistic SF hybrid this state is hard to achieve due to the large resistivity of the F layer). In our work we consider only a Fulde-Ferrell-like state because for the studied system, the LO state has higher energy [21]. In bulk superconductors with a spatially uniform exchange field (magnetic superconductor), the LO state has lower energy, as was found in Ref. [18]. This difference could be connected with the properties of the SFN trilayer, where superconducting and ferromagnetic films are thin, spatially separated, and there is a gradient of superconducting characteristics across the thickness of the trilayer. This brings about a difference even between the properties of Fulde-Ferrell states in the SFN trilayer and the magnetic superconductor. In both systems in the ground state there is a finite phase gradient $\nabla\varphi = \mathbf{q}_{FF}$, but in the SFN structure there are finite superconducting currents flowing in the S and FN layers in opposite directions [16] with the total (thickness integrated) zero current, while in the magnetic superconductor there are no spatially separated currents and both local and total currents are equal to zero.

To calculate the magnetization curve of the SFN strip, we use two models. First, we use the two-dimensional (2D) Usadel equation for normal $g = \cos\Theta$ and anomalous $f = \sin\Theta\exp(i\varphi)$ quasiclassical Green functions [22–24], assuming that Θ depends only on x and y, and we neglect their dependence on the z coordinate,

$$\frac{\hbar D}{2}\left(\frac{\partial^2\Theta}{\partial x^2}+\frac{\partial^2\Theta}{\partial y^2}\right) - \left((\hbar\omega_n + iE_{ex}) + \hbar\frac{D}{2}q^2\cos\Theta\right)\sin\Theta + \Delta\cos\Theta = 0. \tag{1}$$

Here D is the diffusion coefficient of the corresponding layer, E_{ex} is the exchange field, which is nonzero only in the F layer, Δ is the superconducting order parameter, which is nonzero only in the S layer, $\hbar\omega_n = \pi k_B T(2n+1)$ are the Matsubara frequencies (n is an integer number), $q = \nabla\varphi + 2\pi\mathbf{A}/\Phi_0$ is the gauge invariant phase gradient that is proportional to supervelocity $v_s \sim q$ (in this model it has only a z component—see Fig. 1), φ is the phase of the order parameter, $\mathbf{A}$ is the vector potential, and $\Phi_0 = \pi\hbar c/|e|$ is the magnetic flux quantum. Δ should satisfy the self-consistency equation

$$\Delta\ln\left(\frac{T}{T_{c0}}\right) = 2\pi k_B T\sum_{\omega_n>0}\mathrm{Re}\left(\sin\Theta_S - \frac{\Delta}{\hbar\omega_n}\right), \tag{2}$$

where T_{c0} is the critical temperature of a single S layer in the absence of magnetic field. Equation (1) is supplemented by the Kupriyanov-Lukichev boundary conditions between layers [25],

$$D_S\frac{d\Theta_S}{dx}\bigg|_{x=d_S-0} = D_F\frac{d\Theta_F}{dx}\bigg|_{x=d_S+0},$$
$$D_F\frac{d\Theta_F}{dx}\bigg|_{x=d_S+d_F-0} = D_N\frac{d\Theta_N}{dx}\bigg|_{x=d_S+d_F+0}. \tag{3}$$

We assume transparent interfaces between layers, and thereupon Θ is a continuous function of x. For interfaces with vacuum, we use the boundary condition $d\Theta/dn = 0$.

Because the thickness of the whole structure is much smaller than the London penetration depth λ of the single S layer, we neglect the contribution to the vector potential from screening currents. In calculations we use the following vector potential: $\mathbf{A} = (0, 0, -H_\parallel x + H_\perp y)$, where $H_\parallel$ is the parallel and $H_\perp$ is the perpendicular magnetic field (see Fig. 1).

We calculate the magnetization $\mathbf{M}$ as

$$\mathbf{M} = \frac{\mathbf{m}}{dw} = \frac{1}{2cdw}\iint[\mathbf{r}\times\mathbf{j}_s]dx\,dy, \tag{4}$$

where $\mathbf{j}_s = (0, 0, j_z)$ is the superconducting current density,

$$j_z(x,y) = \frac{2\pi k_B T}{e\rho}q\sum_{\omega_n>0}\mathrm{Re}(\sin^2\Theta), \tag{5}$$

and we are interested in the x component of magnetization, M_x.

In the numerical calculations we use dimensionless units. The magnitude of the order parameter is normalized in units of $k_B T_{c0}$, and length is in units of $\xi_c = \sqrt{\hbar D_S/k_B T_{c0}}$. The magnetic field is measured in units of $H_s = \Phi_0/2\pi w\xi_c$, and magnetization M_x is in units of $M_0 = \Phi_0/2\pi\xi_c^2$. We also include in the calculations that $\lambda(0)/\xi_c = 50$, where $\lambda(0)$ is the London penetration depth in a single S layer at $T = 0$.

To find j_z and M_x, we numerically solve Eqs. (1) and (2) with corresponding boundary conditions. To reduce the number of free parameters, we assume that the resistivities of the S and F layers are equal, i.e., $\rho_S/\rho_F = 1$, which corresponds roughly to the parameters of real highly resistive S and F films. We use $\rho_S/\rho_N = 150$ in our calculations because the formation of the FF state in the SFN structure requires a large ratio of resistivities of the N and S layers [16]. It corresponds, for example, to the pair NbN/Au.

The model above is not able to take into account the states with a dependence of Θ on a longitudinal coordinate (for example, a vortex state). To obtain full in-plane distribution of the superconducting order parameter and current density, one has to solve the 3D Usadel equation, which is a complicated problem. Instead, we use the Ginzburg-Landau-like approach

and describe the SFN structure by the 2D (in the y and z directions) equations with the effective superconducting order parameter Ψ averaged over the thickness of the SFN trilayer [20]. The GL free-energy functional describing the 2D superconductor being in the FFLO phase was proposed in Ref. [26],

$$\widetilde{F} = \alpha(T)|\widetilde{\Psi}|^2 + \frac{\beta}{2}|\widetilde{\Psi}|^4 + \gamma(|\Pi_y\widetilde{\Psi}|^2 + |\Pi_z\widetilde{\Psi}|^2) + \delta(|\Pi_y^2\widetilde{\Psi}|^2 + |\Pi_z^2\widetilde{\Psi}|^2 + |\Pi_y\Pi_z\widetilde{\Psi}|^2 + |\Pi_z\Pi_y\widetilde{\Psi}|^2), \tag{6}$$

where $\widetilde{\Psi}$ is a complex superconducting order parameter, and $\Pi_{y,z} = \nabla_{y,z} + i2\pi A_{y,z}/\Phi_0$. One has to define the signs of phenomenological parameters—α, $\gamma < 0$ and β, $\delta > 0$—to have the Fulde-Ferrell state as a ground state [27,28]. We have to stress that for the SFN trilayer this functional was not derived from microscopic theory, and we use it as a phenomenological theory.

The dimensionless free energy F and order parameter Ψ are introduced as $F = F_{\rm GL}\widetilde{F} = (\alpha^2/\beta)\widetilde{F}$, $\Psi = \Psi_0\widetilde{\Psi} = \sqrt{|\alpha|/\beta}\widetilde{\Psi}$, with the characteristic length $\xi_{\rm GL} = \sqrt{|\gamma|/|\alpha|}$ and the dimensionless parameter $\zeta = |\alpha|\delta/|\beta|^2$. Varying $\int F\,dS$ with respect to $\widetilde{\Psi}^*$, we obtain the Ginzburg-Landau equation for the dimensionless order parameter:

$$\zeta\{\Pi_y^4 + \Pi_y^2\Pi_z^2 + \Pi_z^2\Pi_y^2 + \Pi_z^4\}\Psi + \{\Pi_y^2 + \Pi_z^2\}\Psi + \Psi|\Psi|^2 - \Psi = 0. \tag{7}$$

Equation (7) is supplemented by the boundary conditions

$$\Pi\Psi\Big|_n = 0, \quad \Pi^3\Psi\Big|_n = 0, \tag{8}$$

which provide a vanishing of the normal component of superconducting current $j_s|_n$ and supermomentum $q|_n = (\nabla\varphi + 2\pi A/\Phi_0)|_n$ on the boundary of the FF strip with vacuum [20].

In the GL model we find M_x by numerical differentiation of $F_{\rm GL}(H_\perp)$,

$$M_x = -\frac{dF_{\rm GL}}{dH_\perp}. \tag{9}$$

In principle, the same could be done in the Usadel model without use of Eq. (4), but it requires a small step in $H_\perp$ and a very large amount of calculation time. This is why we use different methods to find $M_x(H_\perp)$ in the Usadel and GL models.

We use the relaxation method with addition of the time derivative $\partial\Psi/\partial t$ on the right-hand side of Eq. (7) and looking for $\Psi(y,z)$, which does not depend on time. In numerical calculations, we set $\zeta = 1/8, 1/2, 2, 4$. Case $\zeta \lesssim 1/2$ corresponds to a situation when the coherence length $\xi = \xi_{\rm GL}\{2\zeta/[(1+4\zeta)^{1/2} - 1]\}^{1/2}$ (characteristic length variation of $|\Psi|$ in the used model) is larger than $q_{\rm FF}^{-1} = \xi_{\rm GL}\sqrt{2\zeta}$ while for $\zeta \gtrsim 1/2$ we have the opposite case, which corresponds to properties of the SFN strip with realistic parameters.

III. MAGNETIC RESPONSE OF AN SFN STRIP BEING IN THE FF STATE

In Fig. 2 we present the dependence $M_x(H_\perp)$, found in the Usadel model, for the SFN strips with different widths

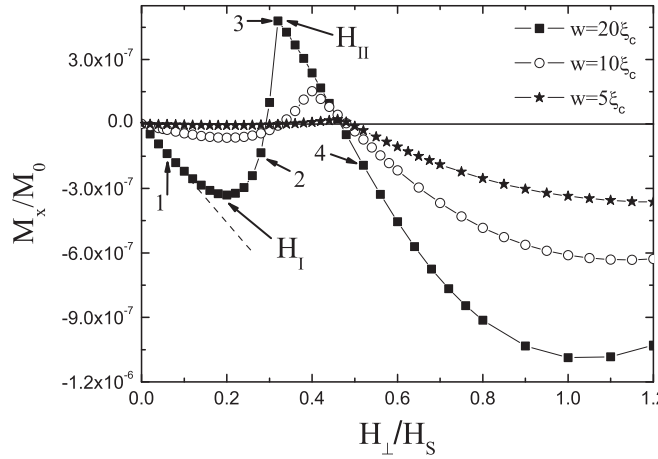

FIG. 2. The magnetization curves of SFN strips with different widths, found from the Usadel model. At $H_\perp = H_I$ there is a local minimum in dependence $M_x(H_\perp)$. At field $H_\perp = H_{\rm II}$ there is a second-order transition from the state with $\overline{q_z} \neq 0$ ($H_\perp < H_{\rm II}$—FF-like state) to the state with $\overline{q_z} = 0$ ($H_\perp \geqslant H_{II}$—ordinary state). Numbers 1–4 indicate fields at which a distribution of sheet current density over the width of the SFN strip is shown in Fig. 3(a). The parameters of SFN strips are as follows: $w = 5, 10, 20\xi_c$; $d_{\rm S} = 1.1\xi_c$; $d_{\rm F} = 0.5\xi_c$; $d_{\rm N} = \xi_c$; $E_{\rm ex} = 5k_BT_{c0}$; and $T = 0.2T_{c0}$.

being in an FF state at $H_\perp = 0$. The magnetic response is diamagnetic at small fields as in ordinary superconductors and magnetic superconductors with a spatially uniform exchange field [17,18], but at some field (we mark it as $H_{\rm I}$ in Fig. 2) M_x reaches a minimal value and then becomes a nonmonotonic function of $H_\perp$ and changes sign twice. As a result, there is a finite range of magnetic fields where magnetic response is paramagnetic. Moreover, at field $H_\perp = H_{\rm II}$ (see Fig. 2) there is a kink, which is a signature of the second-order phase transition from the state with $\overline{q_z} \neq 0$ ($\overline{q_z} = \int q_z dy/w$ is width averaged q_z) to the state with $\overline{q_z} = 0$.

To explain this behavior, in Figs. 3(a) and 3(b) we show the distribution of sheet current density $J_z = \int j_z dx$ and supervelocity $\sim q_z$ over the width of an SFN strip, and in Fig. 4 we show the dependence of $J_z(q_z)$ in a spatially homogeneous case [$q_z(y) = \text{const}$ and $J_z(y) = \text{const}$]. When $H_\perp = 0$ in the ground state of the FF strip there is a finite phase gradient $\nabla\phi = q_{\rm FF}$ but $J_z(q_{\rm FF}) = 0$. From Fig. 4 one can see that near $q_z = q_{\rm FF}$ there is a London-like relation $J_z(y) \sim J_z(q_{\rm FF}) + [2\pi A_z(y)/\Phi_0]dJ_s/dq_z \sim -A_z(y)$, which leads to the diamagnetic response of the FF strip at small fields (see Fig. 2). At that field dependence $J_z(y)$ is a nearly odd function of y [$J_z(y) \sim -J_z(-y)$—see Fig. 3(a) for $H_\perp = 0.06H_s$] as in an ordinary strip because dJ_s/dq_z is almost constant at $q_z \simeq q_{\rm FF}$—see the dashed line in Fig. 4.

At larger fields due to different nonlinearity of $J_z(q_z)$ at $q_z < q_{\rm FF}$ and $q_z > q_{\rm FF}$ the width averaged $\overline{q_z}$ [$\overline{q_z}(H_\perp = 0) = q_{\rm FF}$] decreases, as can be seen from Fig. 3(b), to provide zero full current $\int J_z dy = 0$, and $J_z(y)$ is not an odd function of y [see Fig. 3(a) for $H_\perp = 0.28H_s$]. As a side effect it leads to a nonmonotonous change of $|M_x|$ and even to a paramagnetic response because there is a region ($0 < q_z < q_{c1}$) where $dJ_z/dq_z > 0$. In the current driven regime with $q_z(y) = \text{const}$

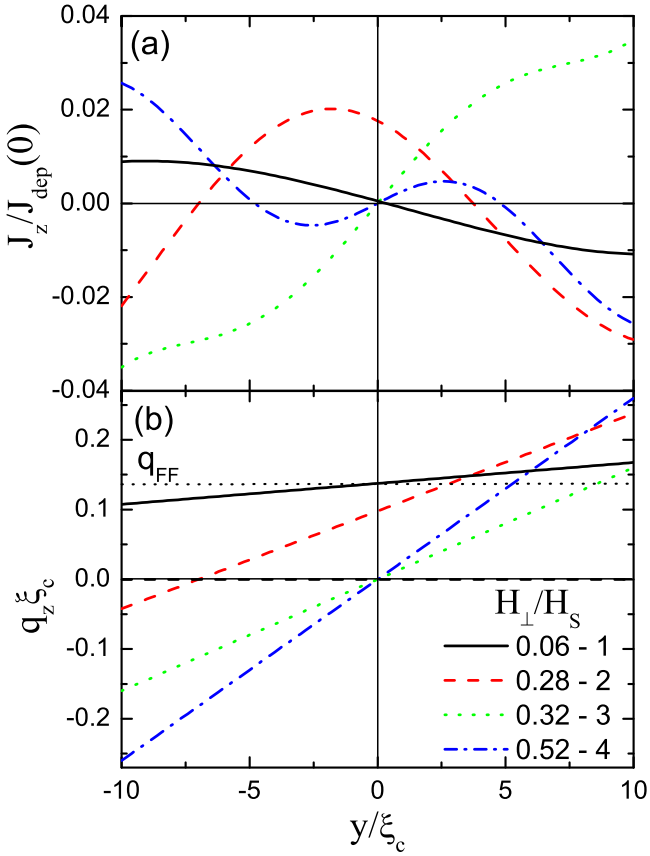

FIG. 3. (a) Distribution of sheet current density J_z and (b) supervelocity $\sim q$ over SFN strip with width $20\xi_c$ at different $H_\perp$ marked by numbers 1–4 in Fig. 2. At $H_\perp = 0.32H_s$ the $\overline{q} = 0$. J_z is normalized in units of $J_{dep}(0) = j_{dep}(0)d$, where $j_{dep}(0)$ is the depairing current density of a single S layer at $T = 0$.

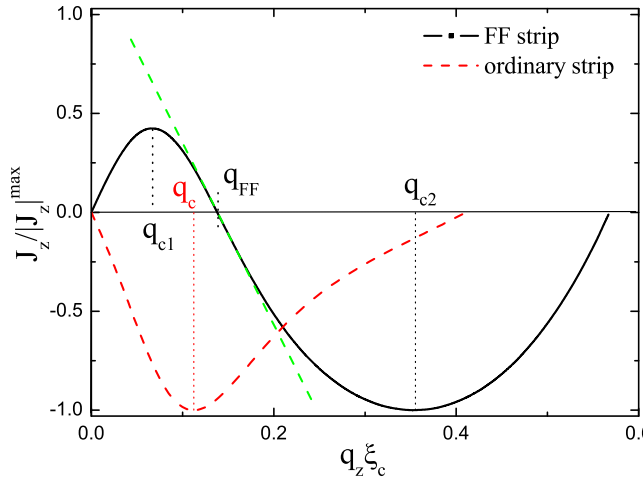

FIG. 4. Dependence of sheet current density J_z on q_z in a spatially uniform case [$J_z(y) = \text{const}$] for SFN strip (parameters as in Fig. 2) being in the FF state and the SFN strip (parameters as in Fig. 2 except $d_F = 0.2\xi_c$) being in an ordinary state. J_z is normalized by critical current density (it corresponds to maximal $|J_z| = |J_z|^{max}$).

this region is not accessible [27] but it can be reached, as we find here, with coordinate-dependent $q_z(y)$.

The $\overline{q_z}$ goes to zero at $H_\perp = H_{II}$ and simultaneously M_x reaches a maximal positive value. M_x decreases and then changes sign at $H_\perp > H_{II}$ while $\overline{q_z} = 0$. Therefore, at $H_\perp = H_{II}$ there is a second-order phase transition from the state with $\overline{q_z} \neq 0$ (Fulde-Ferrell-like state) to the state with $\overline{q_z} = 0$, which is manifested as a kink on $M_x(H_\perp)$ (see Fig. 2).

In an ordinary superconducting strip the vorticities enter the sample when supervelocity at the edge exceeds a critical value [$|\pm q_z(w/2)| \gtrsim q_c$] [29], except for rather narrow strips with $w \lesssim 2\xi(T)$, which do not have space for a vortex [30,31]. We expect similar behavior for the FF strip, which is why we do not present $M_x(H_\perp)$ in Fig. 2 at large fields where $q_z(w/2)$ well exceeds q_{c2} [$q_z(w/2) = q_{c2}$ at $H_\perp = 0.71H_s$ for chosen parameters]. But for the FF strip we have an additional critical value—q_{c1} (see Fig. 4). Note that $q_z(-w/2)$ becomes smaller than q_{c1} (it occurs at $H_\perp \lesssim H_I$) before M_x changes sign, which means that instability may occur, which breaks the homogeneities along the strip state and changes depending on $M_x(H_\perp)$. To check this, we calculate the magnetic response of an FF strip of finite length using the Ginzburg-Landau model.

We find that while the width of the strip is smaller than $w_c \sim 2q_{FF}^{-1}$, the evolution of M_x and $\overline{q_z}$ with magnetic field is similar to that found from the Usadel model [compare Fig. 5(a) and Fig. 2]. There is a range of magnetic fields where the magnetic response is paramagnetic and at $H = H_{II}$ there is second-order transition to a state with $\overline{q_z} = 0$. At larger fields, magnetic response again becomes diamagnetic, and if the width of the strip is larger than $\sim 2\xi$, vortices enter the FF strip, which leads to jumps in M_x as in an ordinary superconducting strip [see Fig. 5(a)]. Moreover, even the relative change of magnetization is similar in Figs. 2 and 5 (if we compare, for example, maximal positive and negative M_x). Note that in Fig. 2 we present results found in the Usadel model for the SFN structure with realistic parameters, and it helps to estimate the strength of the effect (see Sec. IV). In Fig. 5 we present results found in the GL model, where M_{GL} is some parameter that we cannot express via material characteristics of the SFN structure.

For a strip with $w > w_c$, the evolution of M_x and $\overline{q_z}$ in the field range $H_I \lesssim H_\perp \leqslant H_{II}$ is different. It turns out that at $H_\perp \gtrsim H_I$ there appears finite q_y (transversal component of $\vec{q}$) not only near the ends of the strip, where it provides conservation of the full current, but also far from it [see the insets in Fig. 5(b)]. In different halves of the strip, q_y has the opposite sign due to the different sign of the screening currents. In regions where $q_y \neq 0$, $\overline{q_z}$ became suppressed, and it has a maximum in the center of the strip. With increasing magnetic field, $\overline{q_z}(z)$ gradually decreases and at $H = H_{II}$ it goes to zero along the whole strip.

Apparently, the found critical width of the strip $w_c \sim 2q_{FF}^{-1}$ is correlated with the critical length of the quasi-1D FF superconductor $L_c = \pi/\sqrt{2}q_{FF}^{-1} \simeq 2.2q_{FF}^{-1}$ when a spatially modulated state with $q \neq 0$ can appear [20]. In a narrower strip the transition to the state with $\overline{q_z} = 0$ occurs homogenously along the strip because $\overline{q_z}$ depends on z only near the ends where $q_z = 0$ due to boundary conditions, and results found in the framework of the Usadel and GL models qualitatively coincide. In a wider strip, $\overline{q_z}$ strongly depends on length at $H_\perp > H_I$ because of the appearance of a transversal component of $\vec{q}$. Obviously this result cannot be found in the framework of our 2D Usadel model, which assumes spatial uniformity

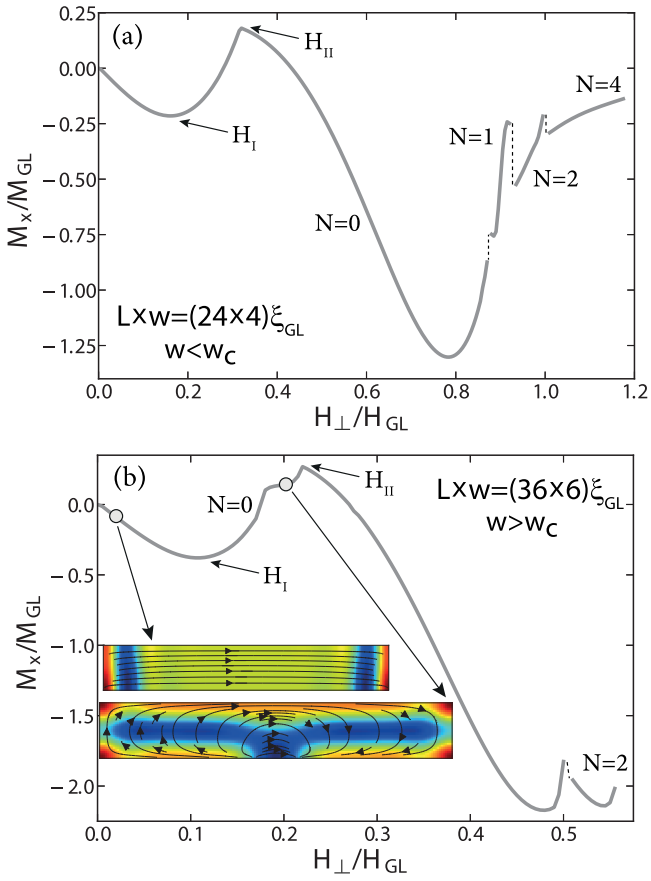

FIG. 5. Field-dependent magnetization of FF strips calculated in the framework of the Ginzburg-Landau model. Lateral sizes of FF strip are shown in panels (a) and (b), parameter $\zeta = 2$ ($q_{FF}^{-1} = 2\xi_{GL} > \xi = \sqrt{2}\xi_{GL}$). Magnetic field is measured in units of $H_{GL} = \Phi_0/2\pi\xi_{GL}^2$, magnetic moment is in units of $M_{GL} = F_{GL}/H_{GL}$, and $N = \oint \nabla\varphi d\mathbf{l}/2\pi$ is a total vorticity in the strip. In the inset in (b) we show the spatial distribution of $|\Psi|$ and q at different magnetic fields.

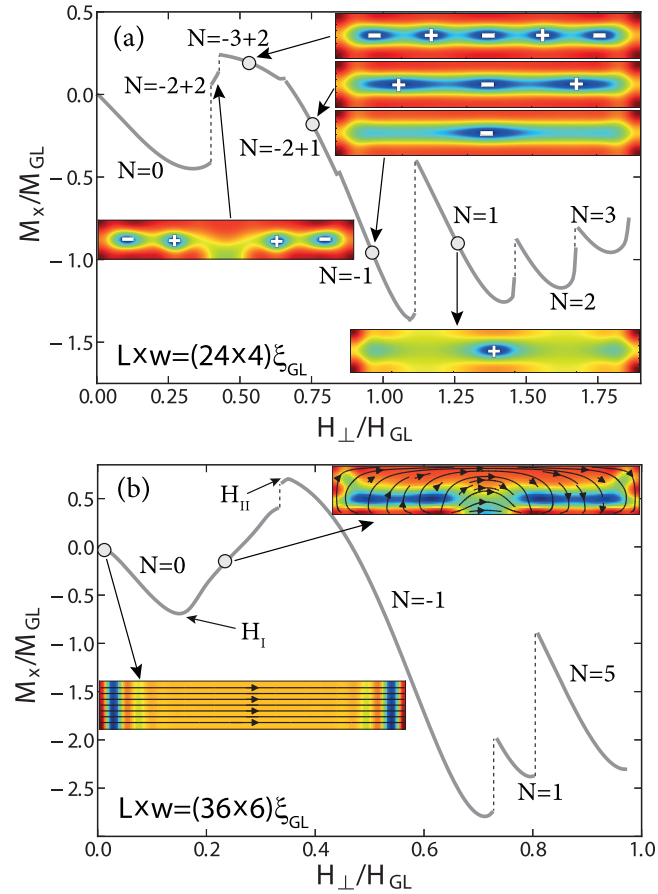

FIG. 6. Field-dependent magnetization of FF strips calculated in the framework of the Ginzburg-Landau model. Lateral sizes of the FF strip are shown in panels (a) and (b), parameter $\zeta = 0.5$ ($q_{FF}^{-1} = \xi_{GL} < \xi \simeq 0.84\xi_{GL}$). For both panels, $w > w_c$. In the insets we show the spatial distribution of $|\Psi|$ and q at different magnetic fields. Symbols − and + indicate antivortex and vortex, respectively.

$[q_z(z) = \text{const}]$ along the FF strip. It leads to a quantitatively different shape of $M_x(H_\perp)$ in a field range $H_I < H_\perp < H_{II}$ for strips with $w > w_c$ and $w < w_c$ [compare Fig. 5(b) with Fig. 5(a) and Fig. 2]. For parameters of the SFN strip, the magnetic response is shown in Fig. 2, $q_{FF}^{-1} \sim 7.2\xi_c$ (see Fig. 4), and hence only for a strip with $w = 20\xi_c$ can we expect the appearance of transversal modulation.

We also find interesting behavior when $\zeta = 1/2$ and $1/8$, which correspond physically to $\xi \gtrsim q_{FF}^{-1}$. In a strip with $w \gtrsim w_c$, the transition to the state with $\overline{q_z} = 0$ starts from the ends of the strip but it is accompanied not only by the appearance of finite q_y but also vortex-antivortex pairs [see the insets in Fig. 6(a)]. In a longer strip their number increases with increasing magnetic field, and it reaches the maximal value at $H = H_{II}$ (for example, when $L = 48\xi_{GL}$ there are four vortex-antivortex pairs—not shown here). At $H = H_{II}$ there is a first-order transition to the state with $\overline{q_z} = 0$ and one additional antivortex enters the strip in its center [see Fig. 6(a)]. With a further increase of magnetic field the number of vortex-antivortex pairs decreases one by one, and at large field only vortices exist in the strip. In a wider strip [see Fig. 6(b)], vortex-antivortex pairs do not appear, but the transition at $H = H_{II}$ is also of first order, and one antivortex enters the strip in its center, which is annihilated with vortices at larger fields [see Fig. 6(b)].

In ordinary superconductors, vortices and antivortices can coexist in small-sized (mesoscopic) samples placed in an external magnetic field [32–34] or near a ferromagnetic domain wall where the magnetic field changes the sign [experimentally such vortices and antivortices have been observed recently in the ferromagnetic superconductor $EuFe_2(As_{0.79}P_{0.21})_2$ [35]]. In zero magnetic field, their simultaneous appearance in the ground state was predicted in an FFLO system with two coupled superconducting order parameters [36], and as a metastable state they may exist in a small-sized FF superconductor [20]. We find that in the FF strip, the vortex-antivortex chain is a ground state in a finite range of the magnetic fields when $w \gtrsim w_c$ and $\xi \gtrsim q_{FF}^{-1}$.

Using the Usadel approach, we also calculate the dependence $M_x(T)$ at fixed $H_\perp$ and $M_x(H_\perp)$ at different temperatures (see Fig. 7). We use the same parameters as in Fig. 2, except the thickness of the S layer was chosen, $d_S = 1.4\xi_c$, for which the transition temperature to the FF state T^{FF} is below the critical temperature of trilayer $T_c = 0.62T_{c0} >$

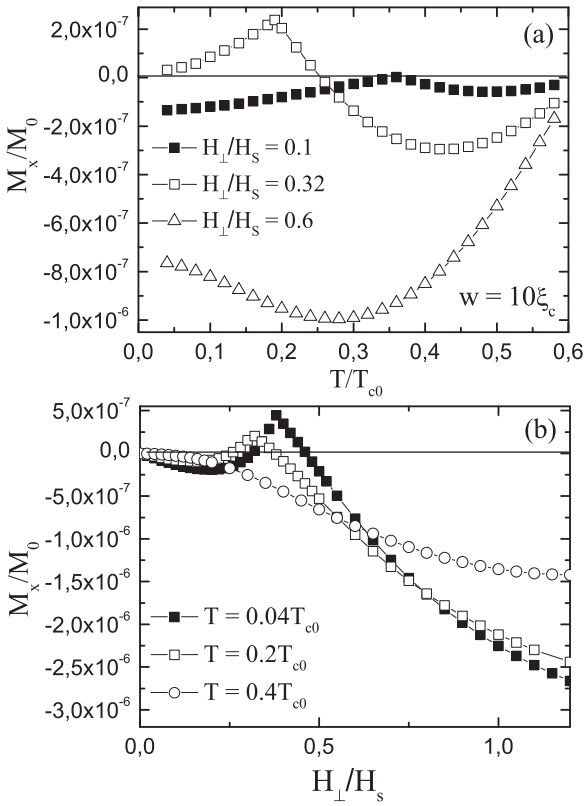

FIG. 7. (a) Dependence of the magnetization of the SFN strip on the temperature at different values of the perpendicular magnetic field. (b) The magnetization curve of the SFN strip at different temperatures. We use the same parameters of the SFN strip as in Fig. 2 except $d_S = 1.4\xi_N$ and choose $w = 10\xi_c$. The temperature of transition to the FF state is $T^{FF} = 0.38T_{c0}$, and the critical temperature of the SFN trilayer is $T_c = 0.62T_{c0}$ (both at $H_\perp = 0$).

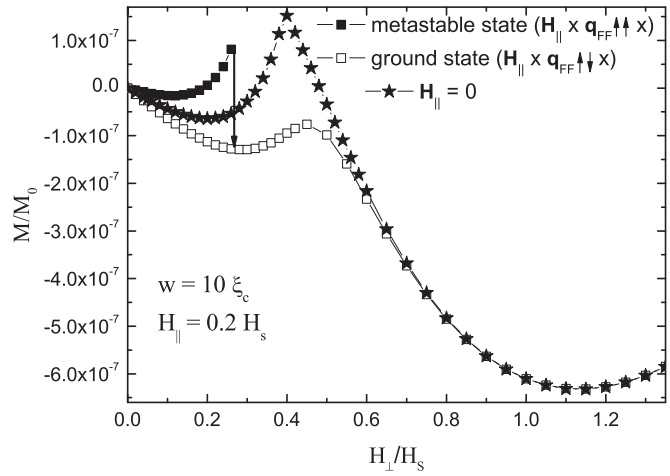

FIG. 8. The magnetization curves of the SFN strip being in ground and metastable FF states (having opposite $\mathbf{q}_{FF}$) which are controlled by a parallel magnetic field. For comparison we also present $M_x(H_\perp)$ when $H_\parallel = 0$. The arrow indicates the direction of magnetization jump which occurs with an increase of $H_\perp$. The width of the SFN strip $w = 10\xi_c$, $H_\parallel = 0.2H_s$, and the other parameters are as in Fig. 2. At $H_\parallel > H_\parallel^* \simeq 0.4H_s$ and $H_\perp = 0$ there is only a state with $H_\parallel \times \mathbf{q}_{FF} \uparrow\downarrow x$.

$T^{FF} = 0.38T_{c0}$. It can be seen that $M_x(T)$ at small fields is nonmonotonous even at $T > T^{FF}$, which is a consequence of the existence of paramagnetic currents in FN layers, while the global magnetic response is diamagnetic for all fields when $T > T^{FF}$ [see Fig. 7(b)].

In the absence of a parallel magnetic field, the ground FF state is twofold-degenerate due to the existence of two states with opposite directions of $\mathbf{q}_{FF}$ along the strip, and for both directions magnetization curves $M_x(H_\perp)$ coincide. In Ref. [21] it was shown that a parallel magnetic field removes this degeneracy and makes the state with $H_\parallel \times \mathbf{q}_{FF} \uparrow\downarrow x$ more favorable while the other state has larger energy (it becomes unstable at relatively low but finite $H_\parallel^*$). This leads to different $M_x(H_\perp)$ for states with opposite $\mathbf{q}_{FF}$ at fixed $H_\parallel$ or vice versa. In Fig. 8 we show this effect. The metastable state becomes unstable at some $H_\perp$, and the SFN strip switches to the ground state. Note that the abrupt change in magnetization is not connected with the vortex entrance or exit, but it occurs due to a change of direction of $\overline{\mathbf{q}}$.

IV. SUMMARY

We show that the SFN strip being in a spatially modulated (Fulde-Ferrell-like) ground state has a global paramagnetic response in a finite range of perpendicular magnetic fields, while at low and large fields the response is diamagnetic. We demonstrate that the found evolution of a magnetic response with increasing magnetic field is accompanied by a vanishing of the width averaged longitudinal phase gradient $\overline{q_z}$, which is equal to q_{FF} at zero magnetic field. We argue that both the paramagnetic response and the vanishing of $\overline{q_z}$ are related, and they are connected with a peculiar dependence of sheet superconducting current density on supervelocity (phase gradient) in the FF state.

In a relatively narrow SFN strip with width $w < w_c \sim 2q_{FF}^{-1}$, the transition from the state with $\overline{q_z} \neq 0$ to the state with $\overline{q_z} = 0$ at field $H_\perp = H_{II}$ is of second order and it occurs uniformly along the strip (except its ends). At this field, the paramagnetic response is maximal. In a wider strip ($w > w_c$) this transition is accompanied by the appearance of spatial modulation of both the phase and magnitude of the superconducting order parameter across the width, which leads to a quantitative modification of the magnetic response. Calculations in the framework of the Ginzburg-Landau model show that the transition of the FF strip with width $w \gtrsim w_c$ and $\xi \gtrsim q_{FF}^{-1}$ to a state with $\overline{q_z} = 0$ starts from the appearance of vortex-antivortex pairs near the ends of the strip and ends with the formation of a vortex-antivortex chain before the first-order transition occurs at $H_\perp = H_{II}$. At fields $H_\perp \gg H_{II}$ both narrow and wide FF strips behave like an ordinary superconducting strip—they have a diamagnetic response, and the number of vortices increases with an increase of $H_\perp$.

A parallel magnetic field removes the degeneracy, connected with two directions of $\mathbf{q}_{FF}$ along the SFN strip. It results in different magnetization curves $M_x(H_\perp)$ depending on the parallel or antiparallel orientation of vector $H_\parallel \times \mathbf{q}_{FF}$ and the normal vector to the surface of the SFN strip.

Using the parameters of NbN as the S layer ($\rho_S = 200\ \mu\Omega\,\text{cm}$, $D_S = 0.5\ \text{cm}^2/\text{s}$, $T_{c0} = 10\ \text{K}$) and those of Au as the N layer ($\rho_N = 2\ \mu\Omega\,\text{cm}$), we can estimate the

geometrical parameters of the SFN strip and the value of the paramagnetic response [any ferromagnetic material could be used as a F layer if it stays ferromagnetic when its thickness is about $\xi_F = (\hbar D_F/E_{ex})^{1/2}$—for example, alloy CuNi [37]]. For chosen materials, $\xi_c = 6.4$ nm and $M_0 = 8$ T. From Fig. 2 it follows that for the SFN strip with $w = 20\xi_c \sim 130$ nm the maximal positive $4\pi M_x$ is of the order of a few tenths of a Gauss. Therefore, to see the predicted effect in the array of SFN strips, a SQUID magnetometer should be used to measure their magnetization curves. We do not believe that a vortex-antivortex chain can exist in the SFN strip because $q_{FF}^{-1} \gg \xi_c \sim \xi$ for this system.

When we calculate $M_x(H_\perp)$, we assume that magnetization of the F layer is not changed. In reality it may vary, and it may make an additional contribution to the magnetic response. One way to solve this problem is to measure $M_x(H\perp)$ above and below T_c and then compare them. The second solution is to choose a magnetic material with in-plane magnetization having no or a small number of domains. To decrease $H_\perp$ one can take a wide FF strip. For example, in [37] a well pronounced 0-π transition was found in a planar NbN/CuNi/NbN Josephson junction with lateral size 10 μm × 10 μm. This result says that at least on this scale CuNi is sufficiently homogeneous. For an FF strip based on NbN/CuNi/Au with a width 1 μm and $\xi_c = 6.3$ nm, we have $H_s \sim 50$ Oe, which is small enough.

ACKNOWLEDGMENTS

The authors acknowledge support from Foundation for the Advancement of Theoretical Physics and Mathematics "Basis" (Grant No. 18-1-2-64-2), Russian Foundation for Basic Research (Project No. 19-31-51019), and Russian State Contract No. 0035-2019-0021.

[1] P. Svelindh, K. Niskanen, P. Norling, P. Nordblad, L. Lundgren, B. Lonnberg, and T. Lundstrom, Anti-Meissner effect in the BiSrCaCuO-system, Physica C **162-164**, 1365 (1989).

[2] S. Riedling, G. Bruchle, R. Lucht, K. Rhberg, H. v. Lhneysen, and H. Claus, Observation of the Wohlleben effect in $YBa_2Cu_3O_{7-\delta}$ single crystals, Phys. Rev. B **49**, 13283 (1994).

[3] D. J. Thompson, M. S. M. Minhaj, L. E. Wenger, and J. T. Chen, Observation of Paramagnetic Meissner Effect in Niobium Disks, Phys. Rev. Lett. **75**, 529 (1995).

[4] A. K. Geim, S. V. Dubonos, J. G. S. Lok, M. Henini, and J. C. Maan, Paramagnetic Meissner effect in small superconductors, Nature (London) **396**, 144 (1998).

[5] M. Sigrist and T. M. Rice, Unusual paramagnetic phenomena in granular high-temperature superconductors—A consequence of d-wave pairing? Rev. Mod. Phys. **67**, 503 (1995).

[6] A. E. Koshelev and A. I. Larkin, Paramagnetic moment in field-cooled superconducting plates: Paramagnetic Meissner effect, Phys. Rev. B **52**, 13559 (1995).

[7] V. V. Moshchalkov, X. G. Qiu, and V. Bruyndoncx, Paramagnetic Meissner effect from the self-consistent solution of the Ginzburg-Landau equations, Phys. Rev. B **55**, 11793 (1997).

[8] F. S. Bergeret, A. F. Volkov, and K. B. Efetov, Josephson current in superconductor-ferromagnet structures with a nonhomogeneous magnetization, Phys. Rev. B **64**, 134506 (2001).

[9] M. Alidoust, K. Halterman, and J. Linder, Meissner effect probing of odd-frequency triplet pairing in superconducting spin valves, Phys. Rev. B **89**, 054508 (2014).

[10] Y. Asano, A. A. Golubov, Y. V. Fominov, and Y. Tanaka, Unconventional Surface Impedance of a Normal-Metal Film Covering a Spin-Triplet Superconductor Due to Odd-Frequency Cooper Pairs, Phys. Rev. Lett. **107**, 087001 (2011).

[11] H. Walter, W. Prusseit, R. Semerad, H. Kinder, W. Ass mann, H. Huber, H. Burkhardt, D. Rainer, and J. A. Sauls, Low-Temperature Anomaly in the Penetration Depth of $YBa_2Cu_3O_7$ Films: Evidence for Andreev Bound States at Surfaces, Phys. Rev. Lett. **80**, 3598 (1998).

[12] A. Di Bernardo, Z. Salman, X. L. Wang, M. Amado, M. Egilmez, M. G. Flokstra, A. Suter, S. L. Lee, J. H. Zhao, T. Prokscha, E. Morenzoni, M. G. Blamire, J. Linder, and J. W. A. Robinson, Intrinsic Paramagnetic Meissner Effect Due to s-Wave Odd-Frequency Superconductivity, Phys. Rev. X **5**, 041021 (2015).

[13] F. B. Muller-Allinger and A. C. Mota, Paramagnetic Reentrant Effect in High Purity Mesoscopic AgNb Proximity Structures, Phys. Rev. Lett. **84**, 3161 (2000).

[14] C. Espedal, T. Yokoyama, and J. Linder, Anisotropic Paramagnetic Meissner Effect by Spin-Orbit Coupling, Phys. Rev. Lett. **116**, 127002 (2016).

[15] S. Mironov, A. Mel'nikov, and A. Buzdin, Vanishing Meissner Effect as a Hallmark of in-Plane Fulde-Ferrell-Larkin-Ovchinnikov Instability in Superconductor-Ferromagnet Layered Systems, Phys. Rev. Lett. **109**, 237002 (2012).

[16] S. V. Mironov, D. Vodolazov, Y. Yerin, A. V. Samokhvalov, A. S. Melnikov, and A. Buzdin, Temperature Controlled Fulde-Ferrell-Larkin-Ovchinnikov Instability in Superconductor-Ferromagnet Hybrids, Phys. Rev. Lett. **121**, 077002 (2018).

[17] P. Fulde and R. A. Ferrell, Superconductivity in a strong spin-exchange field, Phys. Rev. **135**, A550 (1964).

[18] A. I. Larkin and Y. N. Ovchinnikov, Inhomogeneous state of superconductors, Zh. Eksp. Teor. Fiz. **47**, 1136 (1964) [Sov. Phys. JETP **20**, 762 (1965)].

[19] S. I. Suzuki and Y. Asano, Paramagnetic instability of small topological superconductors, Phys. Rev. B **89**, 184508 (2014).

[20] V. D. Plastovets and D. Yu. Vodolazov, Paramagnetic Meissner, vortex, and onion-like ground states in a finite-size Fulde-Ferrell superconductor, Phys. Rev. B **101**, 184513 (2020).

[21] P. M. Marychev and D. Yu. Vodolazov, Tuning the in-plane Fulde-Ferrell-Larkin-Ovchinnikov state in a superconductor/ferromagnet/normal-metal hybrid structure by current or magnetic field, Phys. Rev. B **98**, 214510 (2018).

[22] A. A. Golubov, M. Yu. Kupriyanov, and E. Il'ichev, The current-phase relation in Josephson junctions, Rev. Mod. Phys. **76**, 411 (2004).

[23] A. I. Buzdin, Proximity effects in superconductor-ferromagnet heterostructures, Rev. Mod. Phys. **77**, 935 (2005).

[24] F. S. Bergeret, A. F. Volkov, and K. B. Efetov, Odd triplet superconductivity and related phenomena in superconductor-ferromagnet structures, Rev. Mod. Phys. **77**, 1321 (2005).

[25] M. Yu. Kuprianov and V. F. Lukichev, Influence of boundary transparency on the critical current of "dirty" SS'S structures, Sov. Phys. JETP **67**, 1163 (1988).

[26] A. Buzdin, Y. Matsuda, and T. Shibauchi, FFLO state in thin superconducting films, Europhys. Lett. **80**, 67004 (2007).

[27] K. V. Samokhin and B. P. Truong, Current-carrying states in Fulde-Ferrell-Larkin-Ovchinnikov superconductors, Phys. Rev. B **96**, 214501 (2017).

[28] V. D. Plastovets and D. Y. Vodolazov, Dynamics of domain walls in a Fulde-Ferrell superconductor, JETP Lett. **109**, 729 (2019).

[29] D. Yu. Vodolazov, I. L. Maksimov, and E. H. Brandt, Vortex entry conditions in type-II superconductors. Effect of surface defects, Physica C **384**, 211 (2003).

[30] H. J. Fink, Vortex nucleation in a superconducting slab near a second-order phase transition and excited states of the sheath near H_{c3}, Phys. Rev. **177**, 732 (1969).

[31] D. Saint-James, G. Sarma, and E. J. Thomas, *Type II Superconductivity* (Pergamon Press, Oxford, New York, 1969).

[32] L. F. Chibotaru, A. Ceulemans, V. Bruyndoncx, and V. V. Moshchalkov, Symmetry-induced formation of antivortices in mesoscopic superconductors, Nature (London) **408**, 833 (2000).

[33] A. S. Mel'nikov, I. M. Nefedov, D. A. Ryzhov, I. A. Shereshevskii, V. M. Vinokur, and P. P. Vysheslavtsev, Vortex states and magnetization curve of square mesoscopic superconductors, Phys. Rev. B **65**, 140503 (2002).

[34] V. R. Misko, V. M. Fomin, J. T. Devreese, and V. V. Moshchalkov, Stable Vortex-Antivortex Molecules in Mesoscopic Superconducting Triangles, Phys. Rev. Lett. **90**, 147003 (2003).

[35] V. S. Stolyarov, I. S. Veshchunov, S. Yu. Grebenchuk, D. S. Baranov, I. A. Golovchanskiy, A. G. Shishkin, N. Zhou, Z. Shi, X. Xu, S. Pyon, Y. Sun, W. Jiao, G.-H. Cao, L. Ya. Vinnikov, A. A. Golubov, T. Tamegai, A. I. Buzdin, and D. Roditchev, Domain Meissner state and spontaneous vortex-antivortex generation in the ferromagnetic superconductor $EuFe_2(As_{0.79}P_{0.21})_2$, Sci. Adv. **4**, eaat1061 (2018).

[36] A. Samoilenka, F. N. Rybakov, and E. Babaev, Synthetic nuclear Skyrme matter in imbalanced Fermi superfluids with a multicomponent order parameter, Phys. Rev. A **101**, 013614 (2020).

[37] T. Yamashita, A. Kawakami, and H. Terai, NbN-Based Ferromagnetic 0 and π Josephson Junctions, Phys. Rev. Appl. **8**, 054028 (2017).